Int. J. Heat Mass Transfer. Vol. 22, pp. 691–703
Pergamon Press Ltd. 1979. Printed in Great Britain

PREMIXED BURNING IN DIFFUSION FLAMES— THE FLAME ZONE MODEL OF LIBBY AND ECONOMOS

NORBERT PETERS
Institut für Allgemeine Mechanik, Rheinisch-Westfälische Technische Hochschule, Aachen, Germany

(*Received* 19 *October* 1977 *and in revised form* 3 *October* 1978)

Abstract—The flame zone model proposed by Libby and Economos is shown to be based upon the assumption of a one-step reversible chemical reaction with a large activation energy. The limit of large activation energies is exploited by the method of matched asymptotic expansions and the originally missing relation for the critical freezing temperature—essential for the flame zone model—is derived. It is found that the process of freezing is closely related to the flame propagation in an inhomogeneous mixture. The derivation is general but, following the original paper, the numerical results are presented for a locally similar partly premixed boundary layer diffusion flame. The flame zone is constructed as a two-dimensional region of chemical equilibrium bounded by two infinitely thin non-equilibrium layers that assure the transition to the surrounding frozen flow.

NOMENCLATURE

A, parameter, equation (A24);
b, parameter, equation (39);
B, frequency factor;
C, Chapman-Rubesin-parameter, $\rho\mu/(\rho\mu)_e$;
D, diffusion coefficient;
Da, Damköhler number, equation (14);
c_p, c_{pi}, specific heat capacity, equation (26);
E, activation energy;
f', non-dimensional velocity, y/u_e;
g, non-dimensional total enthalpy, equation (25);
h_i, specific enthalpy of ith species;
h, specific enthalpy;
h_{se}, freestream total enthalpy;
Δh_m, heat of reaction, equation (24);
K_y, equilibrium constant, equation (3);
Le, Lewis number $\rho D c_p/\lambda$;
M, mean molecular weight;
M_i, molecular weight of species;
$\dot{M}_i$, non-dimensional chemical production rate;
m, slope coefficient, equation (53);
n, burning rate coefficient, equation (53);
n_t, order of preexponential temperature dependence;
n_1, n_2, n_3, reaction orders;
n_s, sum of reaction orders, $n_s = n_1 + n_2 - 1$;
p, pressure;
Pr, Prandtl number, $\mu c_p/\lambda$;
R, universal gas constant;
r, reaction rate, equation (2);
r_b, radial distance from axis of symmetry for axisymmetric flow;
s, co-ordinate, equation (A15);
$\tilde{s}$, tangential similarity co-ordinate;
T, absolute temperature;
T_a, non-dimensional activation energy, equation (15);
u, tangential velocity component;
V, non-dimensional normal velocity, $V = 2\tilde{s}[f'\partial\eta/\partial x + \rho v(2\tilde{s})^{-1/2}]/(\partial\tilde{s}/\partial x)$;
v, normal velocity component;
x, tangential co-ordinate;
y, normal co-ordinate;
Y_i, mass fraction of ith species;
$\tilde{Y}_j$, mass fraction of jth element;
Z, equilibrium function, equation (12);
Z_1, Z_2, expansion of the equilibrium function.

Greek symbols

β, non-dimensional free stream pressure gradient;
ε, expansion parameter, equation (36);
ζ, stretched co-ordinate, equation (33);
η, normal similarity co-ordinate, equation (4);
θ, non-dimensional temperature;
κ, exponent, $\kappa = 0$ planar flow, $\kappa = 1$ axisymmetric flow;
λ, thermal conductivity;
Λ_0, eigenvalue of equation (43);
μ, dynamic viscosity of mixture;
ν_i, stoichiometric coefficients (backward minus forward);
ξ, stretched co-ordinate, equation (A17);
ρ, density;
σ, first expansion coefficient of Y_2;
τ, first expansion coefficient of θ;
ϕ, mass fraction ratio of injected mixture.

Subscripts and superscripts

c, critical freezing location;
e, boundary layer edge;
eq, equilibrium flow;
f, frozen flow;
i, ith species;
im, intermediate;

j, jth element;
w, wall;
$(\,)^-$, injected quantity;
$(\,)'$, partial derivative in η-direction.

INTRODUCTION

ANALYSING a hydrogen–oxygen boundary-layer diffusion flame, Libby and Economos [1] proposed to replace the well-known flame sheet model by a flame zone model "based on the concept of a critical temperature to distinguish between regions of frozen and equilibrium flow". The basic concept of the model is the following: in the center of the flame, where the temperature is high, there exists a region of local chemical equilibrium. As the temperature decreases to the sides of the flame down to a critical temperature T_c, the chemical equilibrium can no longer be maintained because the chemical reactions freeze abruptly at this temperature. Thus frozen flow exists immediately adjacent to the equilibrium region.

No definite procedure to calculate the temperature T_c was given in [1], but it was proposed that it corresponds to a kinetically determined temperature such as the ignition temperature. In fact, the freezing temperature was understood as the one parameter that represents the chemical kinetics and its introduction had the immediate advantage to make the chemical kinetics disappear from the equations. Thus the flame zone model was applicable to a flame situation which could not be treated by the flame sheet model: that of a partly premixed diffusion flame. In a boundary layer this flame situation occurs if a fuel/oxidizer mixture rather than pure fuel is injected through a porous surface into an oncoming air stream. Experimentally such a flame has been established for instance by Yamaoka and Tsuji in a stagnation point boundary layer [2, 3].

In jet diffusion flames premixed burning occurs more naturally: In lifted flames there is always a region where the gases are premixed before they will eventually burn in a diffusion flame. If the flame is turbulent the quality of the premixing and the way the flame consumes a certain "unmixedness" is decisive for the rate of turbulent combustion. Under this aspect the underlying idea of local freezing and the way that this is related to premixed burning may contribute to the understanding of turbulent diffusion flames. In particular, as it reintroduces the chemical kinetics, the flame zone model closes the gap between the treatment of premixed and diffusion flames.

However, before the model can be applied to more complex flame situations, the physical condition under which the freezing occurs is to be derived and based upon this, a more rigorous mathematical procedure that determines the freezing temperature is required. In a previous paper [4] on a non-equilibrium flat plate boundary-layer diffusion flame using elementary reactions, the author analysed numerically the structure of the chemical production rates. For some of the reactions he observed an abrupt freezing at two different positions within the boundary layer. This appeared to be related to the flame zone model and it was suggested that the physical justification of the model may be sought by examining the limit of large activation energies. Liñán [5], treating counter flow diffusion flames in the asymptotic limit of large activation energies, seemed to have been aware of this, when he remarked in a footnote that the flame zone model requires a kinetic scheme that differs from the one-step-irreversible reaction that he used. As we will see, a one-step-reversible reaction will be adequate.

The aim of the present paper is to present a physical and mathematical justification of the flame zone model on the basis of an asymptotic analysis. As a reference frame the configuration of Libby and Economos will again be taken up. In particular, the value of the freezing temperature that is determined from the analysis will be of interest and it will be seen that there are two different freezing temperatures on either side of the flame, the temperature T_{c1} on the fuel rich side and the temperature T_{c2} on the fuel lean side. These temperatures do also depend on the ratio of the flow time to the residence time in the boundary layer and thus on the distance from the leading edge.

ANALYSIS

Chemical kinetics

As in [1] a laminar boundary-layer flow over a porous surface will be considered. A premixed hydrogen–oxygen mixture is injected into the boundary layer through the pores of the surface and mixes there with the oncoming air stream. As some of the simplifying assumptions in [1] are not substantial for the subsequent analysis, they will be introduced only at the point where a comparison with the results of [1] is made. On the other hand a specification of the chemical kinetics omitted in [1] is essential: It will be assumed that a one-step reversible reaction takes place between hydrogen (subscript 1) and oxygen (subscript 2) to yield water vapour (subscript 3), while nitrogen (subscript 4) remains inert.

$$2H_2 + O_2 \rightleftarrows 2H_2O. \tag{1}$$

The reaction rate is defined by:

$$r = BT^{n_t} \exp\left(-\frac{E}{RT}\right)\left(\frac{\rho}{M_1}\right)^{n_1}\left(\frac{\rho}{M_2}\right)^{n_2} \times \left(Y_1^{n_1} Y_2^{n_2} - \frac{1}{K_y} Y_3^{n_3}\right), \tag{2}$$

where K_y is an artificial equilibrium constant:

$$K_y = (Y_3^{n_3}/Y_1^{n_1} Y_2^{n_2})_{eq}, \tag{3}$$

which is defined such as to make the last term in equation (2) vanish at local chemical equilibrium. The equilibrium mass fractions in equation (3) are determined by the law of mass action. If the reaction orders were equal to the stoichiometric coefficients of

the combustion reaction, K_y would be the equilibrium constant in terms of the mass fractions. The kinetic expression for a one-step-irreversible reaction is obtained from equation (2) by setting K_y equal to infinity.

Differential equations

In the similarity plane:

$$\tilde{s} = (\rho\mu)_e \int_0^x u_e r_b^{2\kappa}\,\mathrm{d}x$$
$$\eta = u_e r_b^{\kappa}(2\tilde{s})^{-1/2}\int_0^y \rho\,\mathrm{d}y, \tag{4}$$

the boundary-layer equations are in dimensionless form [6] [7]:

continuity:

$$2\tilde{s}\frac{\partial f'}{\partial \tilde{s}} + \frac{\partial V}{\partial \eta} + f' = 0; \tag{5}$$

momentum:

$$2\tilde{s}f'\frac{\partial f'}{\partial \tilde{s}} + V\frac{\partial f'}{\partial \eta} = \beta\left(\frac{\rho_e}{\rho} - f'^2\right) + \frac{\partial}{\partial \eta}\left(C\frac{\partial f'}{\partial \eta}\right); \tag{6}$$

total enthalpy:

$$2\tilde{s}f'\frac{\partial g}{\partial \tilde{s}} + V\frac{\partial g}{\partial \eta} = \frac{\partial}{\partial \eta}\left(\frac{C}{Pr}\frac{\partial g}{\partial \eta}\right) + \frac{u_e^2}{h_{se}}\frac{\partial}{\partial \eta}\left[\frac{C}{Pr}(Pr-1)f'\frac{\partial f'}{\partial \eta}\right] + \frac{\partial}{\partial \eta}\left[\sum_{i=1}^{4}\frac{h_i}{h_{se}}\frac{C}{Pr}\frac{\partial Y_i}{\partial \eta}(Le-1)\right]; \tag{7}$$

species mass fractions:

$$2\tilde{s}f'\frac{\partial Y_i}{\partial \tilde{s}} + V\frac{\partial Y_i}{\partial \eta} = \frac{\partial}{\partial \eta}\left(\frac{CLe}{Pr}\frac{\partial Y_i}{\partial \eta}\right) + \dot{M}_i; \quad (i = 1,2,3,4) \tag{8}$$

element mass fractions:

$$2\tilde{s}f'\frac{\partial \tilde{Y}_j}{\partial \tilde{s}} + V\frac{\partial \tilde{Y}_j}{\partial \eta} = \frac{\partial}{\partial \eta}\left(\frac{CLe}{Pr}\frac{\partial \tilde{Y}_j}{\partial \eta}\right). \quad (j = 1,2) \tag{9}$$

Here it has been assumed that the Lewis numbers of all species are equal. The element mass fraction equations are obtained by summation over the species mass fraction equations using the condition of element conservation during a chemical reaction.

In [1] only equations (6), (7), (9) and $(8)_4$ have been employed. Thus, the chemical kinetics did not come into play (they were replaced by the introduction of the critical freezing temperature). The nondimensional chemical production rate, essential in the present study, is defined by:

$$\dot{M}_i = \frac{2\tilde{s}}{u_e \partial\tilde{s}/\partial x}\frac{\nu_i M_i r}{\rho}, \tag{10}$$

where the stoichiometric coefficients ν_i (backward minus forward) are $\nu_1 = -2$, $\nu_2 = -1$, $\nu_3 = 2$. In order not to restrict the analysis to the hydrogen–oxygen reaction, we carry the ν_i's along and, whenever it appears suitable, we will introduce a negative sign before ν_1 and ν_2 in order to handle with positive coefficients.

Introducing the non-dimensional temperature:

$$\theta = \frac{T}{T_e} \tag{11}$$

and the equilibrium function Z:

$$Z = Y_1^{n_1}Y_2^{n_2} - \frac{1}{K_y}Y_3^{n_3}, \tag{12}$$

the non-dimensional chemical production rate is written:

$$\dot{M}_i = \nu_i\frac{M_i}{M_e}Da\left(\frac{\rho}{\rho_e}\right)^{n_s}\theta^{n_t}\exp\left\{-\frac{T_a}{\theta}\right\}Z. \tag{13}$$

Here the Damköhler number Da and the non-dimensional activation energy are defined:

$$Da = \frac{2\tilde{s}B\rho_e^{n_s}M_eM_1^{-n_1}M_2^{-n_2}T_e^{n_t}}{u_e\partial\tilde{s}/\partial x} \tag{14}$$

$$T_a = E/RT_e, \tag{15}$$

where $n_s = n_1 + n_2 - 1$. It is seen that the Damköhler number, representing the ratio of the residence time to the reaction time, is a function of the station $\tilde{s}$ within the boundary layer. Specifically, for a flat plate boundary layer with constant freestream velocity u_e one obtains:

$$Da = \frac{2xB\rho_e^{n_s}M_eM_1^{-n_1}M_2^{-n_2}T_e^{n_t}}{u_e}, \tag{16}$$

showing that it is proportional to the distance from the leading edge.

The density ratio and the mean molecular weight required in equation (13) may be calculated from:

$$\rho/\rho_e = M/(M_e\theta)$$
$$M = \left(\sum_{i=1}^{4} Y_i/M_i\right)^{-1}. \tag{17}$$

Finally, the boundary conditions of equations (6)–(9) are given by:

$$\eta = 0: \quad f' = 0, \quad V = V_w, \quad g = g_w$$
$$V_w(Y_{iw} - Y_i) = \frac{CLe}{Pr}\frac{\partial Y_i}{\partial \eta} \quad (i = 1\text{–}4) \tag{18}$$

$$\eta \to \infty: \quad f' = 1, \quad g = 1, \quad Y_i = Y_{ie}. \tag{19}$$

Defining the element mass fractions of hydrogen and oxygen by

$$\tilde{Y}_1 = Y_1 + Y_3M_1/M_3,$$
$$\tilde{Y}_2 = Y_2 + Y_3M_2/2M_3, \tag{20}$$

it is seen that equations $(18)_4$ and $(19)_3$ have the same form for the element as for the species mass fractions. For freestream air $Y_{1e} = \tilde{Y}_{1e} = 0$ and $Y_{2e} = \tilde{Y}_{2e} = 0.232$. Since a hydrogen/oxygen mixture is injected at a ratio $\phi = Y_2^-/Y_1^-$, where Y_i^- are the

mass fractions in the reservoir, one obtains in terms of ϕ:

$$Y_1^- = \tilde{Y}_1^- = 1/(1+\phi)$$
$$Y_2^- = \tilde{Y}_2^- = \phi/(1+\phi). \tag{21}$$

Coupling functions

As a reasonable approximation one may assume that the last term in equation (7) can be neglected. This is achieved by assuming $Le = 1$. Then, with the definition:

$$h = \sum_{i=1}^{4} Y_i h_i(T), \tag{22}$$

the temperature is expressed in terms of the enthalpy and of one of the species mass fractions, for example Y_2, by:

$$\mathrm{d}T = \frac{1}{c_p}\mathrm{d}h - \frac{(-\Delta h_m)}{(-\nu_2)M_2 c_p}\mathrm{d}Y_2 + \sum_{j=1}^{2}\left.\frac{\partial T}{\partial \tilde{Y}_j}\right|_{h,Y_2}\mathrm{d}\tilde{Y}_j. \tag{23}$$

As the heat of reaction:

$$\Delta h_m = \sum_{i=1}^{3} \nu_i M_i h_i, \tag{24}$$

is negative for exothermic reactions, a negative sign has been introduced in equation (23). With the definition of the non-dimensional total enthalpy:

$$g = h_{se}(h + u_e f'^2/2), \tag{25}$$

the temperature and its derivatives may be calculated, once the solutions of equations (7) and $(8)_2$ are obtained. Note that by working with the enthalpy the assumption of constant c_p has been avoided and the following relation for the mean specific heat capacity may be used:

$$c_p = \sum_{i=1}^{4} Y_i c_{pi}. \tag{26}$$

The coupling functions for the mass fractions Y_1 and Y_3 are readily obtained as:

$$\mathrm{d}Y_1 = \frac{\nu_1 M_1}{\nu_2 M_2}\mathrm{d}Y_2$$
$$\mathrm{d}Y_3 = \frac{\nu_3 M_3}{\nu_2 M_2}\mathrm{d}Y_2. \tag{27}$$

The reason why the mass fraction of oxygen rather than hydrogen should be used as a reference variable lies in the fact that oxygen is present in both, the injected mixture and the freestream flow.

Asymptotic analysis

It is the aim of this section to derive an equation for the unknown critical freezing temperature. For a given flow condition the Damköhler number Da and the activation energy T_a are known and we expect the non-dimensional freezing temperature θ_c to be a function of these parameters. For this reason we consider the mass fraction equation (8) for species 2, while the temperature and the other mass fractions are determined by the aid of the coupling functions. In order to justify the flame zone model we search for a condition that results in an abrupt transition from equilibrium to frozen flow. Physically it is evident that this transition must pass through chemical non-equilibrium but we expect the non-equilibrium to be confined to a very small region that has the character of a boundary layer. Thus we introduce a small parameter ε, to be defined later, which is a measure for the width of the small transition layer between the equilibrium and the frozen flow. However, in the attempt to expand all terms of equation $(8)_2$ in terms of ε, one immediately faces the problem of how to treat the exponential dependence of the reaction rate upon temperature. From a physical point of view, one realizes that if the reaction rate is to take place at a finite rate, a large activation energy requires a large frequency factor also. As the Damköhler number in our definition may be regarded as a non-dimensionalized frequency factor, we cannot expect it to be independent of the activation energy T_a. Thus, as we expand all variables algebraically in terms of ε, we shall expand the product $Da\exp(-T_a/\theta_c)$ rather than Da itself.

With the definition:

$$Da_c = Da\exp(-T_a/\theta_c), \tag{28}$$

the non-dimensional production term takes the following form:

$$\dot{M}_i = \nu_i \frac{M_i}{M_e} Da_c \left(\frac{\rho}{\rho_e}\right)^{n_s} \theta^{n_t} \times \exp\left[-\frac{T_a}{\theta_c}\left(\frac{\theta_c}{\theta} - 1\right)\right] Z. \tag{29}$$

For $T_a \to \infty$ the exponential term in equation (29) has the limit:

$$\exp\left[-\frac{T_a}{\theta_c}\left(\frac{\theta_c}{\theta} - 1\right)\right] \to \begin{cases} \infty & \text{for } \theta > \theta_c \\ 1 & \text{for } \theta = \theta_c \\ 0 & \text{for } \theta < \theta_c. \end{cases} \tag{30}$$

Since the production rate is balanced by the non-zero left hand side of equation (8), this limit leads to:

(a) chemical equilibrium for $\theta > \theta_c$

$$\text{with} \quad Z = 0,$$
$$\text{i.e.} \quad Y_i = Y_{ieq}, \quad \theta = \theta_{eq}; \tag{31}$$

(b) frozen flow for $\theta < \theta_c$

$$\text{with} \quad \dot{M}_i = 0. \tag{32}$$

Thus the flame zone model of Libby and Economos [1] is implicitly based upon the assumption of a large activation energy. Let us assume that the transition from equilibrium to frozen flow occurs from the right to the left as it is schematically shown in Fig. 1, such that for infinitely large values of T_a equilibrium prevails for $\eta \to \eta_c$ and frozen flow for $\eta < \eta_c$. Then, in order to analyse the non-equilibrium

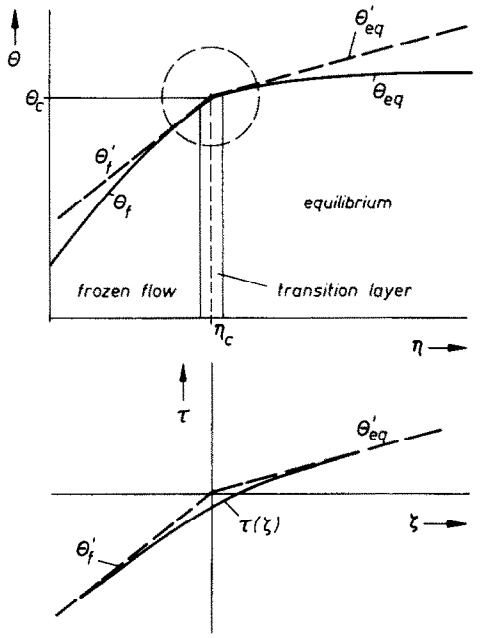

FIG. 1. Schematic representation of the freezing condition and of the transition layer.

transition layer, we stretch the η-co-ordinate around η_c according to

$$\zeta = \frac{\eta - \eta_c}{\varepsilon}. \tag{33}$$

Stretching of the $\tilde{s}$-co-ordinate would be inconsistent with the boundary-layer assumptions and the neglection of the second derivative in $\tilde{s}$-direction. Questions arising at this point will be discussed with the results of the calculation.

In the transition layer the mass fraction Y_2, the temperature and the equilibrium function are expanded in terms of ε as:

$$\begin{aligned} Y_2 &= Y_{2c} + \varepsilon\sigma(\zeta) + \ldots \\ \theta &= \theta_c + \varepsilon\tau(\zeta) + \ldots \\ Z &= Z_c + \varepsilon Z_1(\zeta) + \varepsilon^2 Z_2(\zeta) + \ldots . \end{aligned} \tag{34}$$

Inserting the expansion $(34)_2$ into the exponential term of equation (29)

$$\exp\left[-\frac{T_a}{\theta_c}\left(\frac{\theta_c}{\theta} - 1\right)\right] = \exp\left[\frac{T_a\varepsilon}{\theta_c^2}\tau + \ldots\right], \tag{35}$$

it is seen that a convenient definition of ε is given by:

$$\varepsilon = \theta_c^2/T_a. \tag{36}$$

Thus, in the transition layer $(8)_2$ takes with equations (29) and (33)–(36) the form:

$$\begin{aligned} &2\tilde{s}f'(\eta_c)\varepsilon\frac{\partial\sigma}{\partial\tilde{s}} + V(\eta_c)\frac{\partial\sigma}{\partial\zeta} \\ &= \frac{1}{\varepsilon}\left(\frac{CLe}{Pr}\right)_c\frac{\partial^2\sigma}{\partial\zeta^2} + (-\nu_2)\frac{M_2}{M_e}Da_c\left(\frac{\rho}{\rho_e}\right)^{n_s}\theta_c^{n_t} \\ &\quad\times\exp\tau(Z_c + \varepsilon Z_1 + \varepsilon^2 Z_2\ldots) + O(\varepsilon). \end{aligned} \tag{37}$$

It is seen that the convective terms are of lower order compared to the diffusive term and may thus be neglected. Furthermore, as the equation in the transition layer must join the chemical equilibrium on one side and the frozen flow on the other it is necessary that the chemical production term is retained. This implies that Da_c is at least of order $O(1/\varepsilon^2)$ and that thus to zeroth order the equilibrium function must vanish:

$$Z_c = 0. \tag{38}$$

By comparison with equation (31) this shows that θ_c and Y_{2c} are the equilibrium values at η_c to be determined by the law of mass action.

Now, as we have to deal with a non-premixed system, there are three different orders of magnitude of the ratio Z_1/Z_2 to be considered. From the relations derived in Appendix I, it is seen that this ratio may be expressed in terms of the parameter:

$$b = -\frac{2(\partial Z/\partial\theta)_{eq}}{(\partial^2 Z/\partial\theta^2)_{eq}}. \tag{39}$$

We investigate the following possibilities:

(A) b is of order $O(1)$;
(B) b is of order $O(\varepsilon)$;
(C) b is of order $O(\varepsilon^2)$ or smaller.

It will be seen that the intermediate case includes the two other ones as limiting cases, thus the analysis will be performed for this case only. We write:

$$b = \bar{b}\varepsilon, \tag{40}$$

where $\bar{b}$ is of order $O(1)$, such that Z is expanded as:

$$Z = \varepsilon^2\frac{1}{2}\frac{\partial^2 Z}{\partial\theta^2}\bigg|_{eq}[(\tau - \theta'_{eq}\zeta)^2 - \bar{b}(\tau - \theta'_{eq}\zeta)]\ldots, \tag{41}$$

where the relations derived in Appendix I are used. Here θ'_{eq} denotes the slope of the temperature profile on the equilibrium side of the transition layer at η_c. In Appendix I it is also shown that the only suitable reaction orders are $n_1 = n_2 = 1$. Using these values we expand the Damköhler number Da_c in the following way:

$$\frac{M_2}{M_e}(-\nu_2)Da_c\left[\frac{\rho}{\rho_e}\theta^{n_t}\frac{1}{2}\frac{\partial^2 Z}{\partial\theta^2}\left(-\frac{\partial\theta}{\partial Y_2}\right)\frac{Pr}{CLe}\right]_{\eta_c} = \frac{1}{\varepsilon^3}(\Lambda_0 + \ldots), \tag{42}$$

where Λ_0 is of order $O(1)$. Inserting equations (41)–(42) and (A10) into (37) one obtains:

$$\frac{d^2\tau}{d\zeta^2} = -\Lambda_0[(\tau - \theta'_{eq}\zeta)^2 - \bar{b}(\tau - \theta_{eq}\zeta)]\exp\tau. \tag{43}$$

This equation contains the eigenvalue Λ_0 which is to be determined as a function of $\bar{b}$, θ'_{eq} and the boundary conditions. The boundary conditions are obtained from matching with the outer solutions, i.e. the frozen flow on the left and the equilibrium on the right of the transition layer. As the flame zone model implies that the temperature in the equilibrium region is higher than θ_c, a formal expansion shows that in the limit $T_a \to \infty$ there cannot be any higher

order correction of the local equilibrium solution. Thus, the outer solution on the equilibrium side of the transition layer is given by:

$$\theta = \theta_{eq}(\eta). \tag{44}$$

Also, since the freezing temperature is the equilibrium temperature at η_c, we can expand θ_{eq} around η_c into a Taylor's series:

$$\theta_{eq} = \theta_c + (\eta - \eta_c)\theta'_{eq} \dots . \tag{45}$$

On the frozen flow side one may write the outer expansion:

$$\theta = \theta_f(\eta) + \varepsilon\theta_f^{(1)}(\eta) \dots , \tag{46}$$

where θ_f and $\theta_f^{(1)}$ are solutions of the frozen flow temperature equation, to be derived from equations (7) and $(8)_2$ with the use of coupling functions. The boundary conditions imposed at η_c are obtained from matching with the solution in the transition layer. Matching is affected through introduction of an intermediate variable η_{im} in terms of which η and ζ may be expressed as:

$$\begin{aligned} \eta &= k(\varepsilon)(\eta_{im} - \eta_c) + \eta_c, \\ \zeta &= (\eta_{im} - \eta_c)k(\varepsilon)/\varepsilon, \end{aligned} \tag{47}$$

where $\varepsilon \ll k(\varepsilon) \ll 1$.

Between the frozen flow and the transition layer, the expansions $(34)_2$ and (46) must overlap in the limit;

$$\begin{aligned} \lim[\theta_c + \varepsilon\tau(\zeta) \dots] = &\quad \text{for } \zeta \to -\infty \\ \lim(\theta_f + \varepsilon\theta_f^{(1)} \dots) &\quad \text{for } \eta \to \eta_c. \end{aligned} \tag{48}$$

Expanding θ_f and $\theta_f^{(1)}$ into Taylor's series around η_c, we obtain in terms of η_{im} up to order ε:

$$\theta_f + \varepsilon\theta_f^{(1)} = \theta_f(\eta_c) + k(\varepsilon)(\eta_{im} - \eta_c)\left.\frac{\partial\theta_f}{\partial\eta}\right|_{\eta_c} + \varepsilon\theta_f^{(1)}(\eta_c). \tag{49}$$

The limit (48) yields $\theta_f(\eta_c) = \theta_c$ and procures the boundary condition:

$$\tau = \left.\frac{\partial\theta_f}{\partial\eta}\right|_{\eta_c} \zeta + \theta_f^{(1)}(\eta_c) \quad \text{for } \zeta \to -\infty. \tag{50}$$

If $\theta_f^{(1)}(\eta_c)$ was finite, the solution of equation (43) would depend upon a further unknown parameter with the consequence that the eigenvalue Λ_0 could not be determined. However, let us extend the solution of τ in terms of the outer variables into the frozen flow region. Using equations (33) and $(34)_2$ we obtain:

$$\theta = \theta_c + (\eta - \eta_c)\left.\frac{\partial\theta_f}{\partial\eta}\right|_{\eta_c} + \varepsilon\theta_f^{(1)}(\eta_c), \tag{51}$$

indicating that the flame introduces into the frozen flow solution a perturbation which does not decrease with the distance from the flame. This conflicts with the boundary condition imposed on the frozen flow at $\eta = 0$, which is independent of ε. Thus we obtain $\theta_f^{(1)}(\eta_c) = 0$ and finally the trivial solution $\theta_f^{(1)}(\eta) = 0$. We note that no perturbations are introduced into the frozen flow by the flame.

If the matching procedure is performed on the equilibrium side in the same way, we obtain finally the boundary conditions:

$$\begin{aligned} \tau &= \theta'_f\zeta \quad \text{for } \zeta \rightarrow -\infty, \\ \tau &= \theta'_{eq}\zeta \quad \text{for } \zeta \rightarrow +\infty, \end{aligned} \tag{52}$$

where θ'_f denotes the slope of the frozen flow profile at η_c.

The eigenvalue problem equation (43) with equation (52) bears a close resemblance with equations that have been derived for one-dimensional premixed flames. For instance, in the special case $\theta'_{eq} = 0$ and $\bar{b} = 0$, one obtains the equation that governs the flame propagation in a homogeneous mixture for second order chemical kinetics in the limit of large activation energies [8]. Then Λ_0 is the eigenvalue of the burning rate. If the reaction order is not prescribed and an analysis similar to the present one is performed for the flame propagation in a homogeneous mixture (Appendix II), one obtains equation (43) with $\theta'_{eq} = 0$. In this case equation (43) is readily integrated and the burning rate is obtained as a function of the fuel/oxidizer ratio of the unburnt gas.

As the flame velocity of hydrogen–air mixtures is well known over a wide range of mixture ratios, the kinetic parameters B, n_t and E which appear in the reaction rate (2) as well as in the burning rate formula can be determined by adjustment to experimental data. Thus, the analogy between premixed flames and premixed burning in diffusion flames provides a relation between the freezing temperatures and the measured flame velocities and makes the flame zone model immediately applicable.

A further connection exists between equation (43) and the equation that governs the premixed flame regime that Liñán [5] identified in the analysis of counter-flow diffusion flames. The transformation:

$$\begin{aligned} m &= -\theta'_{eq}/(\theta'_f - \theta'_{eq}), \\ n &= -[\ln 2\Lambda_0 - 2\ln(\theta'_f - \theta'_{eq})]/m, \\ \bar{\tau} &= -\tau + \theta'_{eq}\zeta, \\ \bar{\zeta} &= (\theta'_f - \theta'_{eq})\zeta + n, \end{aligned} \tag{53}$$

casts the problem equation (43) with equation (52) into a form similar to the one that Liñán used. One obtains:

$$\begin{aligned} 2\frac{\mathrm{d}^2\bar{\tau}}{\mathrm{d}\bar{\zeta}^2} &= (\bar{\tau}^2 + \bar{b}\bar{\tau})\exp(-\bar{\tau} - m\bar{\zeta}) \\ \bar{\tau} &= -\bar{\zeta} + n \quad \text{for } \zeta \to -\infty \\ \bar{\tau} &= 0 \quad \text{for } \zeta \to \infty. \end{aligned} \tag{54}$$

Solutions of equation (54) must be sought by numerical integration. Since the objective of the asymptotic analysis is to derive a closed form equation for the freezing temperature, we need to know the dependence of the parameter n, which determines the eigenvalue Λ_0, in terms of m and $\bar{b}$. Using limiting values of m and $\bar{b}$, the following

approximation of a large number of numerical calculations in the range $-10 \geqslant m \geqslant 0$ and $0 \geqslant \bar{b} \geqslant 10$ was obtained:

$$\exp(-mn) = \frac{f_1(m) \cdot f_2(m)}{\bar{b} \cdot f_2(m) + 2 \cdot f_1(m)}, \tag{55}$$

where

$$\begin{aligned} f_1(m) &= 0.6307m^2 - 1.344m + 1 \\ f_2(m) &= -0.56m^3 + 2.36m^2 - 2.1274m + 1. \end{aligned} \tag{56}$$

The constants in equation $(56)_1$ were taken from [5] and the third constant in equation $(56)_2$ from [8]. As no closed form solution of equation (54) could be found in the limit $\bar{b} \to 0$, $m \to -\infty$ the first two constants in equation $(56)_2$ were approximated from the numerical results.

A schematic representation of the entire solution for the temperature profile is given in Fig. 1. In Fig. 1(a) the outer solutions are shown to join each other at η_c with the common value θ_c. The slopes θ'_e and θ'_f are different at this point (they approach each other in the limit $m \to -\infty$), and since an exothermic reaction takes place in the transition layer, the condition $\theta'_f \geqslant \theta'_{eq}$ leads to $m \leqslant 0$. In Fig. 1(b) the solution in the transition layer is shown in terms of τ and the stretched coordinate ζ. The solution τ matches the straight lines which pass through the origin of the τ–ζ coordinate system with the slopes of the outer solutions. If the solution in the transition layer is combined with the outer solutions, it assures a continuous slope of the entire solution and thus a smooth transition from equilibrium to frozen flow.

It is readily seen that the case A is represented by the limit $\bar{b} \to O(1/\varepsilon)$ with equation (42) replaced by

$$\frac{M_2}{M_e}(-\nu_2) Da_c \left(\frac{\rho}{\rho_e} \theta^{n_t} \frac{\partial Z}{\partial Y_2} \frac{Pr}{CLe} \right)_{\eta_c} = \frac{1}{\varepsilon^2}(\bar{\Lambda}_0 + \ldots), \tag{57}$$

where $\bar{\Lambda}_0$ is related to Λ_0 by:

$$\bar{\Lambda}_0 = \Lambda_0 \bar{b}. \tag{58}$$

In this case Liñán's premixed flame regime is recovered. Let us note that according to Appendix II the limit $\bar{b} \to O(1/\varepsilon)$ occurs under either extremely lean or extremely rich mixture conditions only. Case C corresponds to a close-to-stoichiometric mixture, but Fig. 8 shows that $\bar{b}$ approaches the order $O(\varepsilon)$ only in a very narrow region.

It must be stressed that the range of m was restricted to non-positive values. If m was positive, this would imply that there are equilibrium temperatures lower than θ_c. This conflicts with the physical concept of freezing, and following the argumentation that led to equation (44), higher order terms would have to be introduced on the equilibrium side. Liñán considered this case in detail and obtained leakage of both reactants through the flame.

The change of physical significance as m becomes positive is also illustrated by the results of a stability analysis that was performed in [9] for Liñán's premixed flame regime. This analysis showed that Liñán's equation is unstable to small disturbances for $m > 0$ but stable for $m < 0$ and neutrally stable for $m = 0$. When the same sort of stability analysis is performed for the more general problem, equation (54), one obtains the same result. Thus, as m reaches the value zero we expect extinction to occur and in view of equation $(53)_1$ we may deduce a very simple extinction condition for premixed burning in diffusion flames: Extinction occurs if the position of one of the transition layer reaches the temperature maximum.

Finally, the approximation, equations (55)–(56), leads with (23), (28), (41)–(42), (44) and (53) to the following relation in terms of the slopes θ'_{eq} and θ'_f:

$$2Da \exp\left(-\frac{T_a}{\theta_c}\right)\left[\frac{(-\Delta h)_m}{c_p M_e T_e}\frac{\rho}{\rho_e}\theta^{n_t}\frac{Pr}{CLe}\right]_{\eta_c}\left(\frac{\theta_c^2}{T_a}\right)^3 = \bar{f}_1\bar{f}_2\left(-\frac{\partial Z}{\partial\theta}\bigg|_{eq}\frac{T_a}{\theta_c^2}\bar{f}_2 + \frac{\partial^2 Z}{\partial\theta^2}\bigg|_{eq}\bar{f}_1\right), \tag{59}$$

$$\begin{aligned} \bar{f}_1 &= 0.2867\theta'_{eq} - 0.656\theta'_f\theta'_{eq} + \theta'^2_f \\ \bar{f}_2 &= 0.56\theta'^3_{eq}/(\theta'_f - \theta'_{eq}) + 0.2326\theta'^2_{eq} \\ &\quad + 0.1274\theta'_f\theta'_{eq} + \theta'^2_f. \end{aligned}$$

This is the desired equation which determines the freezing temperature θ_c as a function of the Damköhler number Da and the activation energy T_a at every station $\tilde{s}$. Note that since the slopes θ'_{eq} and θ'_f appear always as products, the co-ordinate η may be replaced by $-\eta$ and equation (59) is valid also in the

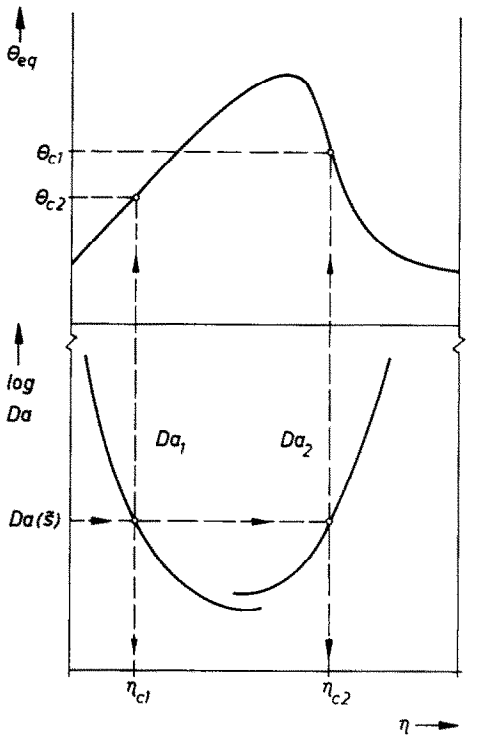

FIG. 2. Schematic representation of the evaluation of equation (59).

case where equilibrium is on the left side of η_c and frozen flow on the right.

As the equation is explicit in the Damköhler number only, but not in θ_c, its evaluation may be performed in the following way, schematically shown in Fig. 2. First, the equilibrium temperature profile is calculated. At every point η the slope θ'_{eq} and the slope θ'_f, that an adjacent frozen flow would have at this particular point, is determined from the solution of equation $(8)_2$ and the coupling function between θ and Y_2. When these values are introduced into equation (59) this results in two curves for the Damköhler number: $Da_1(\eta)$, if the freezing occurs to the left side and $Da_2(\eta)$ if it occurs to the right. Entering into the Da-over-η-plot at the value $Da(\tilde{s})$ which is prescribed according to equation (16) at the particular station $\tilde{s}$, the freezing points η_{c1} and η_{c2} are readily obtained. Moving upwards in Fig. 2 the freezing temperatures θ_{c1} and θ_{c2} are determined. This illustrates also that the freezing temperatures, though of the same order of magnitude, will in general be different.

Furthermore it is seen that in the limit $Da \to \infty$ the freezing points move to the wall and the edge of the boundary layer. Thus the equilibrium model emerges as a special case of the flame zone model in the limit $Da \to \infty$.

RESULTS AND DISCUSSION

In order to demonstrate the use of the formula (59) we will consider the case (a) in [1], which is the most general one, where the freezing occurs on both sides of the flame. Among the various numerical examples presented in [1], those who are plotted in Figs. 13 and 16 with $T_w = 600K$ will be examined in detail. The calculation uses the thermodynamic parameters of Table 2 in [1]. In addition, the kinetic parameters $B_f = 1.08 \times 10^{16}\,\mathrm{cm^3/(mol\,s^{-1})}$, $n_t = 0$ and $E = 30\,\mathrm{kcal\,mol^{-1}}$ derived in Appendix II along with $n_1 = n_2 = 1$ will be used.

The calculation procedure follows closely the one presented in [1], as far as the calculation of the flowfield, the enthalpy and the element mass fractions is concerned. Thus the assumptions $Le = Pr = C = 1$, $\beta = 0$, V_w = constant and local similarity are used in spite of the non-similarity effects imposed by the production rate. The calculation is performed for various values of $\tilde{s}$, so that a freezing contour rather than freezing points will be obtained in the $\tilde{s}$-η-plane.

The following straight forward procedure will be employed:

(1) The element mass fraction profiles are calculated;
(2) The freezing point η_{c1} is prescribed;
(3) The oxygen mass fraction at the wall and the wall enthalpy are calculated with equations (42) and (44) given in [1]. (Note that the indices 1 and 2 are to be interchanged and that there should be a sign of multiplication between the two lines of equation (44) instead of a + sign);
(4) With the wall enthalpy known, the enthalpy profile is given and the equilibrium solution is calculated using the law of mass action, i.e. equations (40) and (41) in [1].

Now, the formula (59) may be evaluated. To do this:

(5) The slope of the equilibrium temperature profile is calculated by the use of a finite difference formula and the slope θ'_f is obtained by differentiating equation (43) in [1] and the use of coupling functions;
(6) This determines $Da_1(\eta_{c1})$ and according to equation (16) the distance x from the leading edge;
(7) Finally, in the same way the second freezing point is obtained by calculating the curve $Da_2(\eta)$ and interpolating such that $Da_1 = Da_2$.

This procedure is shown in Fig. 3 for $\eta_{c1} = 1.0$ resulting in $g_w = -0.1417$ and $Da_1 = 2.466 \times 10^7$, $x = 0.5038m$. The freezing temperatures are $\theta_{c1} = 1.585$ and $\theta_{c2} = 1.791$. The temperature profile in the upper part of Fig. 3 shows a temperature maximum at $\eta = 3.75$ while the flame sheet model, assuming complete combustion, would result in a singular maximum at the location of stoichiometric mixture $\eta_{st} = 4.13$. Since there is practically no fuel present in the frozen flow region on the right hand side of η_{c2}, the frozen flow temperature profile differs very little from the equilibrium profile. On the contrary, the freezing on the fuel rich side at η_{c1} exhibits the true character of premixed burning, and the frozen flow temperature profile (dotted line) is quite different from the equilibrium temperature profile. This is due to the fact that a partly premixed stream is injected into the boundary layer at the wall.

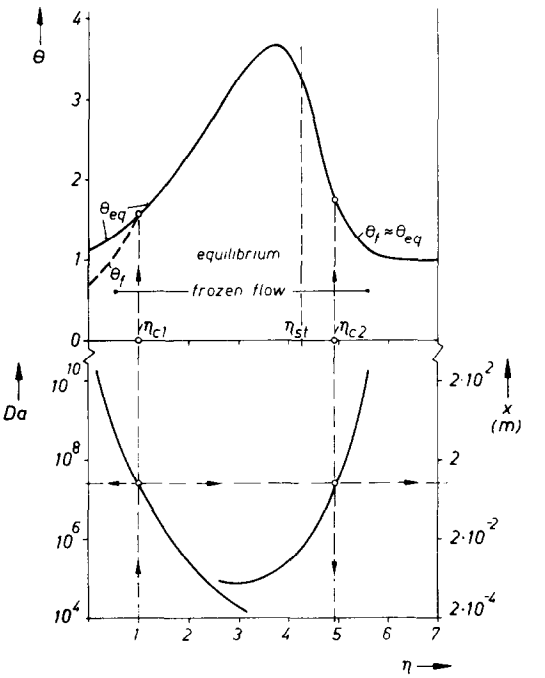

FIG. 3. Temperature profile and Da-numbers for $\eta_{c1} = 1.0$.

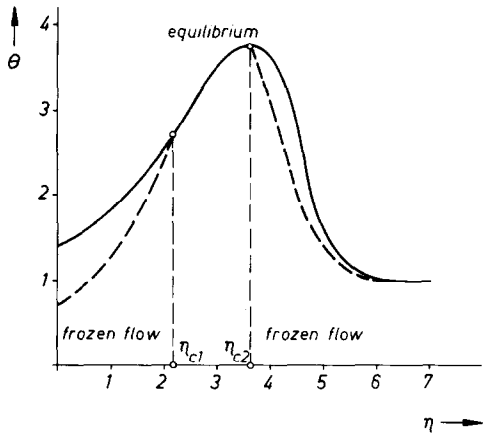

FIG. 4. Temperature profile for $\eta_{c1} = 2.2$.

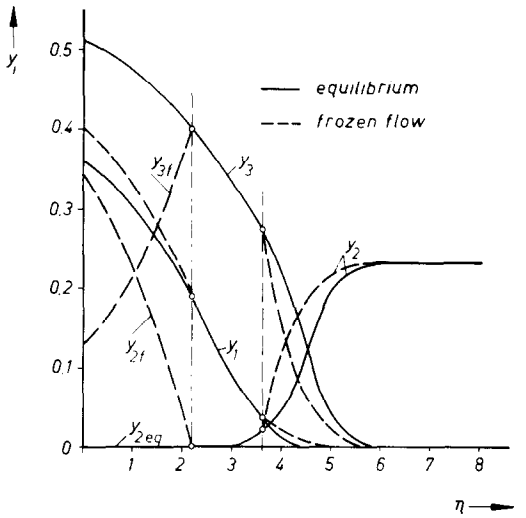

FIG. 5. Mass fraction profiles for $\eta_{c1} = 2.2$.

When the calculation is repeated for larger values of η_{c1}, the Damköhler number (and thus x) decreases and both freezing points move to higher freezing temperatures. For $\eta_{c1} = 2.2$ one obtains $g_w = -0.031$, $Da_1 = 9.8 \times 10^4$ and $x = 2\,\text{mm}$, $\eta_{c2} = 3.62$, $\theta_{c1} = 2.77$ and $\theta_{c2} = 3.75$. Here the second freezing point is close to the temperature maximum. The temperature and mass fraction profiles in Figs. 4 and 5 show a deviation between the equilibrium and frozen flow solutions in both frozen flow regions. The mass fraction of H_2O peaks at $\eta_{c1} = 2.2$ rather than at $\eta_{st} = 4.13$ as would be predicted by the flame sheet model. If local chemical equilibrium was assumed everywhere (equilibrium model), the Y_3-profile has a maximum at the wall, since the injected oxygen is immediately consumed to yield water.

In Fig. 6 the boundaries of the equilibrium region η_{c1} and η_{c2} and the value $(1-g_w)$, which is a measure for the heat transfer to the wall, are plotted over the logarithm of the Damköhler number (the corresponding values of x are shown on the top of the figure). As one moves from large to lower values of Da, the equilibrium region becomes smaller. From

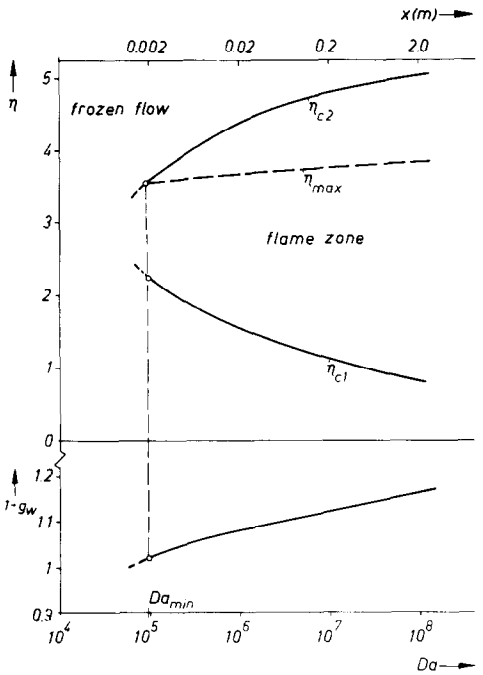

FIG. 6. Two-dimensional flame zone and wall heat transfer.

the lower part of Fig. 6 it is seen that the heat transfer increases as the flame zone approaches the wall. At the intersection of the line of maximum temperature η_{max} with η_{c2} the second transition layer becomes unstable since m has the value zero. Thus no stable flame zone can exist for Damköhler numbers lower than $Da_{min}(x_{min})$. We must keep in mind that due to the boundary-layer assumptions, which neglect diffusion in x-direction, we deal with a flame that propagates in η-direction only. Thus in a flat plate flow we have to take care that the flame has already been stabilized upstream and that stable burning is assured at least up to the position x_{min}. This can be done by placing an obstacle into the boundary layer that reduces the tangential flow locally to values lower than the flame velocity and thus acts as a flame holder.

The situation is somewhat different in a blunt body flow. In this case we would have to consider first the stagnation point boundary layer where the principal flow direction is normal to the surface. There we would obtain a plot of η_{c1} and η_{c2} over Da similar to Fig. 6, but the Damköhler number is then formed with the freestream velocity gradient du_e/dx (instead of u_e/x) and the minimum Damköhler number defines the maximum velocity gradient for which a stable flame can be obtained. Any increase beyond this value would then result in an extinction of the flame in the stagnation point region. When this happens, the flame will be swept downstream and, due to the parabolic character of the boundary-layer flow, it can be stabilized in the wake of the body only.

Let us note that the physical concept of Liñán's premixed flame regime differs from the present one in the following way: the flame zone model is restricted

to the case where an equilibrium region is bounded by two transition layers, while Liñán's premixed flame regime assumes a single layer where the frozen flow covers the region of stoichiometric mixture. The two models join each other, except for the kinetics, for case (b) considered in [1]. In this case the freestream temperature is higher than the freezing temperature and equilibrium is maintained in the outer part of the boundary layer. This corresponds to Liñán's case $2\beta > 1$ where m is negative resulting in a stable transition layer.

CONCLUSIONS

1. The concept of a critical freezing temperature is equivalent to the concept of flame propagation within an inhomogeneous medium. The flame zone that exists in the center of a diffusion flame may be interpreted as an equilibrium region generated between two flame fronts that move in an opposite direction away from each other. This flame propagation requires, that the equilibrium temperature is equal or higher than the temperature in the flame front, otherwise the flame propagation would be unstable.

The concept of freezing temperature has the advantage to include the case where the premixing is low with the burning being stabilized by the heat transfer from the equilibrium region. In the limiting case of a non-premixed system a freezing temperature can still be defined, but then the frozen and equilibrium temperature profiles become identical.

2. The flame zone model uses more physical information than the flame sheet model and is also somewhat more difficult to handle. In exchange, it provides more realistic results, and it should replace the flame sheet model in all cases where premixing is important. In particular, in flames close to extinction the information provided by finite chemical kinetics will be essential.

3. Finally, the analogy between the process of freezing and flame propagation provides realistic kinetic parameters and an insight into the accuracy that may be expected by this one-step-reaction model.

REFERENCES

1. P. A. Libby and C. Economos, A flame zone model for chemical reaction in a laminar boundary layer with application to the injection of hydrogen–oxygen mixtures, *Int. J. Heat Mass Transfer* **6**, 113–128 (1963).
2. I. Yamaoka and H. Tsuji, The structure of rich fuel–air flames in the forward stagnation region of a porous cylinder. *Fifteenth Symposium (International) on Combustion*, pp. 637–644. The Combustion Institute, Pittsburgh (1975).
3. I. Yamaoka and H. Tsuji, Structure analysis of rich fuel–air flames in the forward stagnation region of a porous cylinder. *Sixteenth Symposium (International) on Combustion*, pp. 1145–1154. The Combustion Institute, Pittsburgh (1977).
4. N. Peters, Analysis of a laminar flat plate boundary-layer diffusion flame, *Int. J. Heat Mass Transfer* **19**, 385–393 (1976).
5. A. Liñán, The asymptotic structure of counter flow diffusion flames for large activation energies, *Acta astr.* **1**, 1007–1039 (1974).
6. P. M. Chung, Chemically reacting non-equilibrium boundary layers, *Adv. Heat Transf.* **2**, 109–270 (1965).
7. F. G. Blottner, Finite-difference methods of solutions of the boundary-layer equations, *AIAA Jl* **8**, 193–205 (1970).
8. F. A. Williams, A review of some theoretical considerations of turbulent flame structure, *AGARD* CP-164 (1975).
9. N. Peters, On the stability of Liñán's "Premixed flame regime", *Combust. Flame.*
10. I. B. Zeldovich, Theory of flame propagation, *NACA Techn. Memo.* 1282 (1951).
11. B. P. Mullins and S. S. Penner, Explosions, detonations, flammability and ignition, AGARDOgraph 31, p. 201. Pergamon Press (1959).
12. J. B. Fenn and M. J. Calcote, Activation energies in high temperature combustion, *Fourth Symposium (International) on Combustion*, pp. 231–239. Williams and Wilkins (1953).
13. T. G. Scholte and P. B. Vaags, The burning velocity of hydrogen–air mixtures and mixtures of some hydrocarbons with air, *Combust. Flame* **3**, 495–501 (1959).

APPENDIX I

The expansion coefficients Z_1 and Z_2 of the equilibrium function Z are defined as:

$$Z_1 = \left.\frac{dZ}{d\varepsilon}\right|_{\varepsilon=0}, \quad Z_2 = \frac{1}{2}\left.\frac{d^2Z}{d\varepsilon^2}\right|_{\varepsilon=0}. \tag{A1}$$

Since any function in equation (34) may be expressed in terms of θ and η we write at $\eta = \eta_c$:

$$Z_1 = \left.\frac{\partial Z}{\partial\theta}\right|_{\eta_c}\left.\frac{\partial\theta}{\partial\varepsilon}\right|_{\varepsilon=0} + \left.\frac{\partial Z}{\partial\eta}\right|_{\theta_c}\left.\frac{\partial\eta}{\partial\varepsilon}\right|_{\varepsilon=0}. \tag{A2}$$

As all partial derivatives are to be evaluated at η_c where $\theta = \theta_c$ is an equilibrium value, we replace the indices by the common index eq. From $Z(\theta_c, \eta_c) = 0$ we obtain:

$$\left.\frac{\partial Z}{\partial\eta}\right|_{eq} = -\left.\frac{\partial\theta}{\partial\eta}\right|_{eq}\left.\frac{\partial Z}{\partial\theta}\right|_{eq} \tag{A3}$$

and thus with equations (33)–(34)

$$Z_1 = \left.\frac{\partial Z}{\partial\theta}\right|_{eq}\left(\tau - \left.\frac{\partial\theta}{\partial\eta}\right|_{eq}\zeta\right). \tag{A4}$$

A first differentiation for Z_2 yields:

$$Z_2 = \frac{1}{2}\frac{\partial}{\partial\varepsilon}\left(\left.\frac{\partial Z}{\partial\theta}\right|_{eq}\tau + \left.\frac{\partial Z}{\partial\eta}\right|_{eq}\zeta\right)_{\varepsilon=0}. \tag{A5}$$

As we consider the case B, where $Z_\theta = (\partial Z/\partial\theta)_{eq}$ is of order $O(\varepsilon)$ we get similarly:

$$\left.\frac{\partial Z_\theta}{\partial\varepsilon}\right|_{\varepsilon=0} = \left.\frac{\partial^2 Z}{\partial\theta^2}\right|_{eq}\left(\tau - \left.\frac{\partial\theta}{\partial\eta}\right|_{eq}\zeta\right) \tag{A6}$$

and further

$$\frac{\partial}{\partial\varepsilon}\left(\left.\frac{\partial Z}{\partial\eta}\right|_{eq}\right)_{\varepsilon=0} = -\left.\frac{\partial\theta}{\partial\eta}\right|_{eq}\left.\frac{\partial^2 Z}{\partial\theta^2}\right|_{eq}\left(\tau - \left.\frac{\partial\theta}{\partial\eta}\right|_{eq}\zeta\right), \tag{A7}$$

where the relation (A3) and

$$\frac{\partial}{\partial\theta}\left.\frac{\partial Z}{\partial\eta}\right|_{eq} = \left.\frac{\partial Z_\theta}{\partial\eta}\right|_{eq} = -\left.\frac{\partial\theta}{\partial\eta}\right|_{eq}\left.\frac{\partial^2 Z}{\partial\theta^2}\right|_{eq} \tag{A8}$$

was used. Thus we obtain for Z_2:

$$Z_2 = \frac{1}{2}\left.\frac{\partial^2 Z}{\partial\theta^2}\right|_{eq}\left(\tau - \left.\frac{\partial\theta}{\partial\eta}\right|_{eq}\zeta\right)^2. \tag{A9}$$

Also, using the coupling function between T and Y_2 we obtain for σ:

$$\sigma = \left.\frac{dY_2}{d\varepsilon}\right|_{\varepsilon=0} = \left.\frac{\partial Y_2}{\partial\theta}\right|_{eq}\tau + \left.\frac{\partial Y_2}{\partial\eta}\right|_{eq}\zeta. \tag{A10}$$

The partial derivative of the equilibrium function Z with respect to temperature at chemical equilibrium is:

$$\left.\frac{\partial Z}{\partial\theta}\right|_{eq} = \left(n_1 Y_1^{n_1-1} Y_2 \frac{\partial Y_1}{\partial\theta} + n_2 Y_1^{n_1} Y_2^{n_2-1}\frac{\partial Y_2}{\partial\theta} + \frac{1}{K_y^2}\frac{\partial K_y}{\partial\theta} Y_3^{n_3} - \frac{n_3}{K_y} Y_3^{n_3-1}\frac{\partial Y_3}{\partial\theta}\right)_{eq}. \tag{A11}$$

While the two terms of the equilibrium function are equal by definition, in the derivatives the last terms containing the equilibrium constant K_y are dominated by the terms containing Y_1 and Y_2. From (A11) we see further, that in order to avoid physically meaningless singularities in the second derivative, the reaction orders $n_1 = n_2 = 1$ are suggested. This leads to:

$$\left.\frac{\partial Z}{\partial\theta}\right|_{eq} = \left(Y_2\frac{\partial Y_1}{\partial\theta} + Y_1\frac{\partial Y_2}{\partial\theta}\right)_{eq} \tag{A12}$$

and to the second derivative:

$$\left.\frac{\partial^2 Z}{\partial\theta^2}\right|_{eq} = \left(Y_2\frac{\partial^2 Y_1}{\partial\theta^2} + 2\frac{\partial Y_1}{\partial\theta}\frac{\partial Y_2}{\partial\theta} + Y_1\frac{\partial^2 Y_2}{\partial\theta^2}\right)_{eq}. \tag{A13}$$

These equations simplify further in the case of a very lean ($Y_{1eq} \ll 1$) or very rich ($Y_{2eq} \ll 1$) mixture. The partial derivatives with respect to the temperature, as obtained from the coupling functions, involve the heat of reaction.

APPENDIX II

The steady, one-dimensional, plane, laminar flame propagation at constant pressure in a homogeneous mixture is described under the assumption of a one-step-reversible reaction by the solution of the equation:

$$(\rho v)_F\frac{dY_1}{dx} = \frac{d}{dx}\left(\rho D\frac{dY_1}{dx}\right) + \nu_1 M_1 r, \tag{A14}$$

$$Y_1 = Y_{1-\infty} \quad \text{for } x \to -\infty$$
$$Y_1 = Y_{1eq} \quad \text{for } x \to +\infty,$$

where equation (2) and the coupling functions are to be used. Here $(\rho v)_F$ is the mass burning rate to be determined. In terms of the co-ordinate

$$s = \exp\int_0^x \frac{(\rho v)_F}{\rho D}\,dx, \tag{A15}$$

the equation reduces with $n_1 = n_2 = 1$ to

$$s^2\frac{d^2Y_1}{ds^2} = \frac{(-\nu_1)BT^{n_t}\rho^3 D}{(\rho v)_F^2 M_2}\exp\left(-\frac{T_a}{\theta}\right)Z. \tag{A16}$$

Here the temperature has been non-dimensionalized by the adiabatic flame temperature T_{eq}.

The location of the flame is given by $s = 1$. In the limit of large activation energies one introduces the expansion (34) and obtains in terms of the stretched co-ordinate

$$\zeta = \frac{s-1}{\varepsilon}, \tag{A17}$$

by the same procedure as above:

$$\frac{d^2\tau}{d\zeta^2} = -\Lambda_0(\tau^2 - \bar{b}\tau)\exp\tau \tag{A18}$$

where Λ_0 is given by:

$$\frac{(-\nu_1)B\exp(-T_a)}{(\rho v)_F^2 M_2}\left[T^{n_t}\rho^3 D\frac{1}{2}\frac{\partial^2 Z}{\partial\theta^2}\left(-\frac{\partial\theta}{\partial Y_1}\right)\right]_{eq} = \frac{1}{\varepsilon^3}(\Lambda_0 + \ldots) \tag{A19}$$

Matching with the outer solutions:

$$\begin{aligned} Y_\Lambda &= Y_{1-\infty} + s(-Y_{1-\infty} + Y_{1eq}) \quad 0 \leqslant s \leqslant 1 \\ Y_\Lambda &= Y_{1eq} \qquad\qquad\qquad\qquad s \geqslant 1, \end{aligned} \tag{A20}$$

yields the boundary conditions

$$\begin{aligned} \tau &= \left.\frac{\partial\theta}{\partial Y_1}\right|_{eq}(Y_{1eq} - Y_{1-\infty})\xi \quad \text{for } \xi - \infty \\ \tau &= 0 \qquad\qquad\qquad\qquad\qquad\quad \text{for } \xi + \infty. \end{aligned} \tag{A21}$$

When (A18) is integrated between $\xi = -\infty$ and $\xi = +\infty$ one obtains

$$\left[\left.\frac{\partial\theta}{\partial Y_1}\right|_{eq}(Y_{1eq} - Y_{1-\infty})\right]^2 = 2\Lambda_0(\bar{b}+2). \tag{A22}$$

With $\theta = 1$ and the approximation

$$(\partial^2 Z/\partial\theta^2)_{eq} = 2(\partial Y_1/\partial\theta)_{eq}(\partial Y_2/\partial\theta)_{eq}$$

this leads finally to the burning rate formula

$$(\rho v)_F = A\left\{2BT_{eq}^{n_t}(\rho^3 D)_{eq}\exp\left(-\frac{E}{RT_{eq}}\right)\left[\frac{(-\nu_1)Y_{2eq}}{M_2} + \frac{2\nu_1\nu_2 c_{peq}RT_{eq}^2}{E(-\Delta h_m)_{eq}} + \frac{(-\nu_2)Y_{1eq}}{M_1}\right]\right\}^{1/2} \tag{A23}$$

where the coefficient A:

$$A = \frac{c_{peq}RM_1T_{eq}^2(-\nu_1)}{E(-\Delta h_m)_{eq}(Y_{1-\infty} - Y_{1eq})} \tag{A24}$$

reduces for constant Δh_m and c_p to

$$A = \frac{RT_{eq}^2}{E(T_{eq} - T_{-\infty})}. \tag{A25}$$

This formula is a generalized form of the burning rate formula derived by an order-of-magnitude analysis by Zeldovich and Frank-Kamenetzki [10]. It includes his formula for first and second order reaction as special cases. It will be evaluated for the hydrogen–oxygen reaction with the aim to determine B, n_t and E by comparison with measured flame velocities. The result of this comparison is at the same time a measure of the accuracy that may be obtained by the use of one-step-reaction kinetics.

Extremely different values of the activation energy are reported in the literature: From ignition temperatures, Mullins and Penner [11] obtained a value of 57 kcal mol^{-1} while Fenn and Calcote [12] got a value of 16 kcal mol^{-1} from an empirical relationship between the activation energy and the lean limit flame temperature in flame propagation measurements. These two values were inserted with $n_t = 0$ into (A23)–(A24) and B was adjusted in order to give a maximum flame velocity of 2.75 m s^{-1}. The comparison with the measured flame velocities of Scholte and Vaags [13] in Fig. 7 shows that the peak of the theoretical burning velocities occurs at about 32% H_2, where the equilibrium temperature has a maximum, rather than at 43% H_2 obtained from the measurements. The 57 kcal mol^{-1}-curve approaches the measurements better on the lean side, while the 16 kcal mol^{-1}-curve is better on the rich side. As a compromise we adopt the value $E =$ 30 kcal mol^{-1} resulting in $B = 1.08 \times 10^{16}$ cm^3 mol^{-1} s^{-1}. The shift of the maximum to the rich side is probably due to the influence of diffusion. The diffusion coefficient of H_2 in N_2 is about 3 times greater than that of O_2 in N_2, and in rich H_2 flames the excess H_2 will enhance the burning rate. This could be corrected by introducing a mixture dependent diffusion coefficient, but since this effect is particular to the combustion of hydrogen, while the aim of the analysis is more general, we do not want to complicate the equations.

It is interesting to consider the relative influence of the three terms in square brackets in (A23) as well as the coefficient $\bar{b}$ which is the quotient of the sum of the first and third to the second term. Figure 8 shows that the first term vanishes in fuel rich and the third term in fuel lean mixtures, while the second term varies mainly in the same

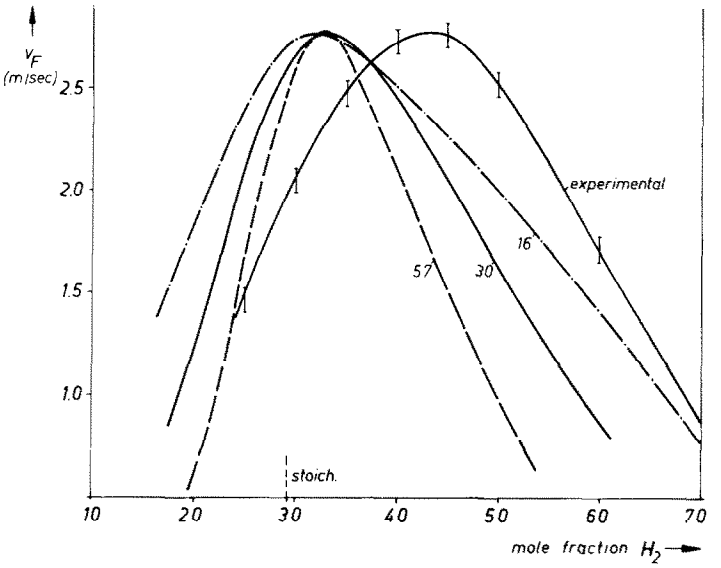

FIG. 7. Experimental and predicted flame velocities.

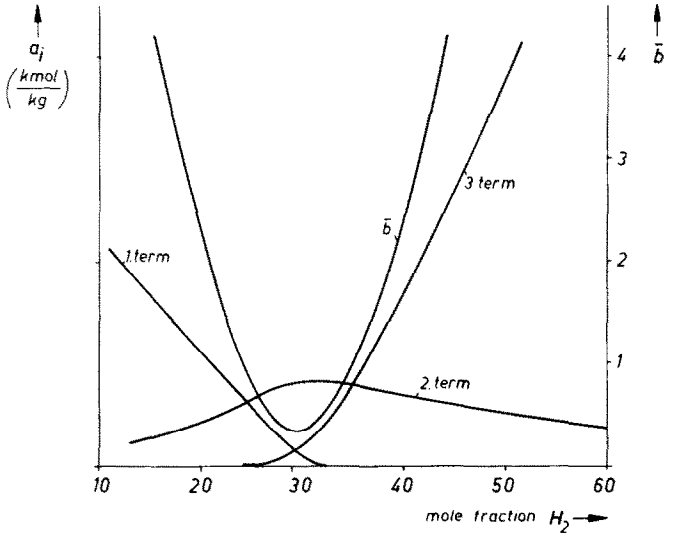

FIG. 8. Comparison of the different terms in (A23).

way as the square of the equilibrium temperature, having a flat maximum at about 32% H_2. Consequently, $\bar{b}$ has a minimum of about 0.35, to be compared to $\varepsilon \approx 0.16$, at the stoichiometric mixture and it attains large values for very lean or very rich mixtures. This indicates that to prescribe the reaction order is essentially an assumption about the fuel/oxidizer ratio. In very lean or very rich mixtures only the deficient reactant controls the burning rate and this corresponds to a reaction order one for this reactant. In a close-to-stoichiometric mixture both reactants are rate determining leading to a reaction order two in the Zeldovich–Frank–Kamenetsky formula.

COMBUSTION AVEC PREMELANGE DE FLAMMES DE DIFFUSION LE MODELE DE LA ZONE DE FLAMME DE LIBBY ET ECONOMOS

Résumé—On montre que le modele de la zone de flamme proposé par Libby et Economos est basé sur l'hypothèse d'une réaction chimique réversible avec une grande énergie d'activation. La limitation aux énergies d'activation grandes est exploitée par la méthode des développements asymptotiques et on établit la relation manquante de la température critique de figeage, essentielle au modèle de la zone de flamme. On montre que le processus de figeage est étroitement relié à la propagation de la flamme dans un mélange non-homogène. Le traitement est général mais, en suivant l'article original, les résultats numériques sont présentés pour une flamme de diffusion prémélangée en couche limite avec similitude locale. La zone de flamme est construite comme une région bidimensionnelle d'équilibre chimique, limitée par deux couches infiniment minces hors d'équilibre qui assurent la transition avec l'écoulement gelé environnant.

VORGEMISCHTE VERBRENNUNG IN DIFFUSIONSFLAMMEN—DAS FLAMMENZONENMODELL VON LIBBY UND ECONOMOS

Zusammenfassung—Für das von Libby und Economos vorgeschlagene Flammenzonenmodell wird gezeigt, das es auf der Annahme einer Ein-Schritt-Reaktion mit einer großen Aktivierungsenergie beruht. Der Grenzfall großer Aktivierungsenergien wird mit Hilfe der Methode der angepaßten asymptotischen Entwicklungen behandelt und die ursprünglich fehlende Beziehung für die Einfriertemperatur, die wesentlich für das Flammenzonenmodell ist, wird hergeleitet. Es stellt sich heraus, daß der Einfrierprozeß mit der Flammenausbreitung in einem inhomogenen Gemisch verwandt ist. Die Herleitung ist allgemein, die numerischen Ergebnisse werden jedoch in Anlehnung an die Originalarbeit für eine örtlich ähnliche, teilweise vorgemischte Grenzschicht-Diffusionsflamme dargestellt. Die Flammenzone wird als ein zweidimensionales Gleichgewichtsgebiet konstruiert, das durch zwei unendlich dünne Nichtgleichgewichtsschichten begrenzt ist, die den Übergang zur umgebenden eingefrorenen Strömung sicherstellen.

ГОРЕНИЕ ПРЕДВАРИТЕЛЬНО СМЕШАННЫХ КОМПОНЕНТОВ В ДИФФУЗИОННЫХ ФАКЕЛАХ. ЗОНАЛЬНАЯ МОДЕЛЬ ПЛАМЕНИ ЛИББИ И ЭКОНОМОСА

Аннотация — Показано, что зональная модель пламени, предложенная Либби и Экономосом, основана на допущении наличия одноступенчатой обратимой химической реакции при большой величине энергии активации. Методом сращивания асимптотических разложений с использованием предела больших энергий активации выведено соотношение для критической температуры замораживания, которое ранее не использовалось в зональной модели пламени, но которое является весьма существенным для данной модели. Найдено, что процесс замораживания тесно связан с процессом распространения пламени в неоднородной смеси. Представлены численные результаты для предварительно частично перемешанного диффузионного пламени в локально подобном пограничном слое. Зона факела представлена как двумерная область химического равновесия, ограниченная двумя бесконечно тонкими неравновесными слоями, которые свидетельствуют о наличии перехода в окружающий замороженный поток.